

# Variation of the Nucleation Energy of Molybdenum Silicides as a Function of the Composition of an Amorphous Precursor

Christopher D. Johnson, Kane Anderson, Adam D. Gromko, and David C. Johnson\*

Contribution from the Department of Chemistry and Materials Science Institute, University of Oregon, Eugene, Oregon 97403

Received January 20, 1998

**Abstract:** Modulated elemental reactants containing alternating elemental layers of molybdenum and silicon with overall thicknesses less than 50 Å were found to crystallize various molybdenum silicides depending on their compositions. Modulated reactants with compositions near 1:2 Mo:Si formed  $\beta$ -molybdenum disilicide at 400 °C, even though  $\beta$ -molybdenum disilicide is metastable with respect to  $\alpha$ -molybdenum disilicide below 1900 °C. The activation energy of the nucleation event was found to be 1.9 eV. Modulated reactants with compositions near 5:3 Mo:Si formed  $\text{Mo}_5\text{Si}_3$  at 650 °C with an activation energy of 3.0 eV. Modulated reactants with compositions near 3:1 crystallize  $\text{Mo}_3\text{Si}$  at 750 °C with an activation energy of 2.2 eV. Low-angle X-ray diffraction indicates that significant interdiffusion occurs during annealing below the formation temperatures of the compounds. Transmission electron microscopy data collected on samples annealed below the formation temperatures indicate that the samples were amorphous. The nucleation energy of the compounds was observed to increase as the stoichiometry of the amorphous phase varied from that of the nucleating compound. This implies that the ability to control the crystalline product using the composition of the amorphous intermediate results from the composition dependence of the nucleation energy for crystallization. Presumably,  $\beta$ - $\text{MoSi}_2$  forms because the nucleation barrier is lower than that of the thermodynamically more stable  $\alpha$ - $\text{MoSi}_2$ .

## Introduction

The reactivities of molybdenum–silicon interfaces and multilayers have been the subject of numerous papers in the last 30 years. This interest results from the potential uses of the silicides in applications such as the use of films of  $\text{MoSi}_2$  as protective layers in oxidizing environments,<sup>3</sup> the use of thin silicide layers either as active electronic materials or as diffusion barriers in the semiconductor industry<sup>4</sup> and the use of the multilayer structures themselves as X-ray optical elements in synchrotron radiation beam lines.<sup>1,2</sup> A major concern, however, in determining the feasibility of these applications has been the control of phase formation at the interfaces. Initial reports on the reactivity of relatively thick films of molybdenum on silicon and thick multilayer structures have disagreed with respect to the sequence of phase formation resulting in a number of subsequent investigations.<sup>3–13</sup>

The initial motivation for the study of the reactivity of metal silicon interfaces was the desire to form ohmic or rectifying

(1) Stearns, D. G.; Rosen, R. S.; Vernon, S. P. *J. Vac. Sci. Technol. A* **1991**, *9*, 2662–2669.

(2) Kortright, J. B.; Joksich, S.; Ziegler, E. *J. Appl. Phys.* **1991**, *69*, 168.

(3) Bartlett, R. W.; Gage, P. R.; Larssen, P. A. *Trans. Metall. Soc. AIME* **1964**, *230*, 1528–1534.

(4) Guivarch, A.; Auvray, P.; Berthou, L.; Le Cun, M.; Boulet, J. P.; Henoc, P.; Pelous, G.; Martinez, A. *J. Appl. Phys.* **1978**, *49*, 233–237.

(5) Liang, J. M.; Chen, L. J. *J. Appl. Phys.* **1996**, *79*, 4072–4077.

(6) Stearns, D. G.; Stearns, M. B.; Cheng, Y.; Stith, J. H.; Ceglio, N. M. *J. Appl. Phys.* **1990**, *67*, 2415–2427.

(7) Jiang, Z.; Jiang, X.; Liu, W.; Wu, Z. *J. Appl. Phys.* **1989**, *65*, 196–200.

(8) Nakajima, H.; Fujimori, H.; Koiwa, M. *J. Appl. Phys.* **1988**, *63*, 1046–1051.

(9) Holloway, K.; Do, K. B.; Sinclair, R. *J. Appl. Phys.* **1989**, *65*, 474–480.

(10) Petford-Long, A. K.; Stearns, M. B.; Chang, C. H.; Nutt, S. R.; Stearns, D. G.; Ceglio, N. M.; Hawryluk, A. M. *J. Appl. Phys.* **1987**, *61*, 1422–1428.

contacts to silicon for a variety of electronic applications.<sup>14</sup> The low resistivity (20–25  $\mu\Omega$  cm) and high melting point (2047 °C) of tetragonal  $\alpha$ - $\text{MoSi}_2$  make it a leading candidate for such applications in integrated-circuit interconnection schemes. In most of these studies of metal silicon interfaces, the samples were in the form of metal films deposited on crystalline silicon substrates. In general, kinetics was found to dominate initial compound formation. The molybdenum–silicon system is typical of the systems investigated. For thin molybdenum films deposited upon oxide free silicon surfaces, several groups found that hexagonal  $\beta$ - $\text{MoSi}_2$  was the first compound formed at the reacting interface at a temperature of 500 °C.<sup>4,9,12,13,15</sup> The hexagonal  $\beta$ - $\text{MoSi}_2$  was found to transform to tetragonal  $\alpha$ - $\text{MoSi}_2$  at temperatures above 800 °C. One group reported observing  $\text{Mo}_3\text{Si}$  at the reacting interface when they still had reacting Mo.<sup>8</sup> The surprising reactivity of metal–silicon interfaces at low temperatures and the importance of kinetics in determining which compound would form resulted in empirical rules proposed by several groups to explain the observed reaction kinetics.<sup>16–21</sup>

(11) Sloof, W. G.; Loopstra, O. B.; de Keijser, T. H.; Mittemeijer, E. J. *Scr. Metall.* **1986**, *20*, 1683–1687.

(12) Baglin, J.; Dempsey, J.; Hammer, W.; d'Heurle, F.; Petersson, S.; Serrano, C. *J. Electron. Mater.* **1979**, *8*, 641–661.

(13) Rosen, R. S.; Stearns, D. G.; Viliardos, M. A.; Kassner, M. E.; Vernon, S. P.; Cheng, Y. *Appl. Opt.* **1993**, *32*, 6975–6980.

(14) Tsaor, B. Y.; Lau, S. S.; Mayer, J. W.; Nicolet, M.-A. *Appl. Phys. Lett.* **1981**, *38*, 922–924.

(15) Cheng, J. Y.; Cheng, H. C.; Chen, L. J. *J. Appl. Phys.* **1987**, *61*, 2218–2223.

(16) d'Heurle, F. M. *J. Mater. Res.* **1988**, *3*, 167–194.

(17) d'Heurle, F. M.; Gas, P. *J. Mater. Res.* **1986**, *1*, 205–221.

(18) Walser, R. M.; Bené, R. W. *Appl. Phys. Lett.* **1976**, *28*, 624–625.

(19) Ottaviani, G.; Nobili, C. *Thin Solid Films* **1988**, *163*, 111–121.

(20) Ottaviani, G. *Thin Solid Films* **1986**, *140*, 3–21.

(21) Pretorius, R. *Mater. Res. Soc. Symp. Proc.* **1984**, *25*, 15–20.

**Table 1.** Summary of Previous Investigations of the Mo–Si System<sup>a</sup>

author	deposn technique	sample struct	first compd nucleated	$E_n$ (eV), $T$ (°C), $D$ (cm <sup>2</sup> /s)
Guivarch <sup>4</sup>	sputtered	800 Å Mo on Si	h-MoSi <sub>2</sub>	2.4 eV, growth at 500 °C
Baglin <sup>12</sup>	e-beam	500 Å Mo on Si	h-MoSi <sub>2</sub>	500 °C
Sloof <sup>11</sup>	sputtered	8 Å repeats	h-MoSi <sub>2</sub>	2–300 °C, $1.7 \times 10^{-22}$ cm <sup>2</sup> /s
Petford-Long <sup>10</sup>	sputtered	70–120 Å repeats		interfaces, 10 and 20 Å thick
Nakajima <sup>8</sup>	sputtered	38–76 Å repeats	Mo <sub>3</sub> Si	550 °C
Holloway <sup>9</sup>	sputtered	130 Å repeats	h-MoSi <sub>2</sub>	400 °C, $1.9 \times 10^{-24}$ cm <sup>2</sup> /s 500 °C, $7 \times 10^{-15}$ cm <sup>2</sup> /s 2 eV growth
Jiang <sup>7</sup>		120 Å repeats	Mo <sub>5</sub> Si <sub>3</sub>	600 °C
Stearns <sup>6</sup>	sputtered	110 Å repeats	h-MoSi <sub>2</sub> Mo <sub>5</sub> Si <sub>3</sub> h-MoSi <sub>2</sub> t-MoSi <sub>2</sub>	400 °C, $3 \times 10^{-18}$ cm <sup>2</sup> /s
Rosen <sup>13</sup>	sputtered	70 Å	h-MoSi <sub>2</sub>	2.5 eV
Liang <sup>5</sup>	e-beam	60–70 Å	Mo <sub>5</sub> Si <sub>3</sub> Mo <sub>3</sub> Si	
Chi <sup>38</sup>	sputtered	750 Å repeats	h-MoSi <sub>2</sub> t-MoSi <sub>2</sub>	1.5 eV 7.8 eV
Cheng <sup>15</sup>	e-beam	one bilayer	h-MoSi <sub>2</sub>	570 °C, $1 \times 10^{-16}$ cm <sup>2</sup> /s

<sup>a</sup>  $E_n$  = nucleation energy;  $T$  = formation temperature;  $D$  = diffusion coefficient.

In the mid 1980s, several groups began to look at modulated molybdenum silicon structures as potential X-ray optical elements.<sup>1,22,23</sup> Since one of the proposed uses was as the first optical element, an X-ray reflector, in high-power synchrotron beam lines, several groups reported the interdiffusion rates as a function of temperature while other groups examined the structural degradation of the multilayer structure as a function of temperature and time.<sup>8,9,11,24</sup> For molybdenum–silicon multilayers, interdiffusion, measured using the decay of the (000) satellite diffraction peaks, was observable beginning at 400 °C.<sup>8</sup> The formation of either hexagonal MoSi<sub>2</sub> or Mo<sub>3</sub>Si was observed at the reacting interfaces. Cross-sectional transition electron microscopy (TEM) studies showed the presence of an amorphous interfacial region between Mo and Si in as-deposited multilayers.<sup>9,13</sup> The amorphous interfacial region was between 17 and 10 Å thick, depending on whether Mo was being deposited on Si or Si on Mo, respectively. For samples prepared in ultrahigh vacuum and annealed at 400 °C for 20 min, Mo<sub>3</sub>Si and Mo<sub>5</sub>Si<sub>3</sub> were observed (using TEM) to form in the amorphous region at the reacting interfaces.<sup>5</sup> A summary of previous studies of the reaction between Mo and Si films is contained in Table 1.

Molybdenum–silicon interfaces have also been the subject of fundamental interest and were an important test case for the study of solid-state amorphization reactions. Solid-state amorphization is a process where an amorphous phase grows at a reacting interface. The growth of the amorphous phase is thought to be driven by the large negative heat of mixing. The formation of crystalline equilibrium compounds is frustrated by the kinetic constraints imposed by low reaction temperatures. TEM experiments on Mo–Si multilayers revealed the presence of very thin amorphous layers.<sup>9,13</sup> There is disagreement in the literature on whether a solid-state amorphization reaction occurs. TEM and low-angle X-ray experiments by Holloway et al. showed that the amorphous layers did not grow upon annealing, but instead the amorphous layers crystallized forming binary silicides.<sup>9</sup> This agreed with calculations by Bene who predicted that the amorphization reaction would not occur in molybdenum–silicon interfaces because the energy of the amorphous alloy would not be lower than that of a mechanical mixture of the

elements at any temperature.<sup>25</sup> These calculations were based upon the approach of Miedema and model the amorphous alloy as an undercooled liquid.<sup>26</sup> Rosen et al. present TEM evidence that the amorphous interlayers grow on low-temperature annealing, followed by nucleation of hexagonal MoSi<sub>2</sub> within the amorphous layers.<sup>13</sup>

We have used solid-state amorphization reactions as the first step in a synthesis approach in which we attempt to avoid stable binary compounds as reaction intermediates.<sup>27</sup> We have shown that if we can generate amorphous reaction intermediates of approximately uniform composition, the rate-limiting step in crystalline compound formation is nucleation.<sup>28</sup> The composition of the amorphous intermediate may possibly lead to control of the relative nucleation energies of crystalline compounds.<sup>29</sup> The considerable scatter of literature results combined with the relatively thick repeat thicknesses used in the previous multilayer studies (40–120 Å) prompted us to reinvestigate the reactivity of molybdenum–silicon films. We wondered whether a critical layer thickness existed below which interfacial nucleation could be avoided. We also were interested in whether nucleation energies varied as a function of composition, if composition of the amorphous phase controlled nucleation of compounds, and if this could explain the variety of results reported in the literature with respect to the sequence of phase formation. These questions are part of a more general theme of research in solid-state chemistry, probing which phase nature chooses to form from a given set of atoms at a particular stoichiometry. Developing this understanding will hopefully lead to the ability to rationally prepare new compounds with desired structures.

## Experimental Section

The multilayer samples were prepared in a high-vacuum evaporation system which has been described in detail elsewhere.<sup>30</sup> Briefly, the elements were sequentially deposited in high vacuum (approximately  $5 \times 10^{-7}$  Torr) under computer control. The elements were deposited

(25) Bene, R. W. *J. Appl. Phys.* **1987**, *61*, 1826–1833.

(26) Miedema, A. R.; Niessen, A. K. *Physica* **1982**, *114B*, 367–374.

(27) Novet, T.; Johnson, D. C. *J. Am. Chem. Soc.* **1991**, *113*, 3398–3403.

(28) Fukuto, M.; Hornbostel, M. D.; Johnson, D. C. *J. Am. Chem. Soc.* **1994**, *116*, 9136–9140.

(29) Oyelaran, O.; Novet, T.; Johnson, C. D.; Johnson, D. C. *J. Am. Chem. Soc.* **1996**, *118*, 2422–2426.

(30) Fister, L.; Li, X. M.; Novet, T.; McConnell, J.; Johnson, D. C. *J. Vac. Sci., Technol. A* **1993**, *11*, 3014–3019.

(22) Barbee, T. W., Jr. *MRS Bull.* **1990**, 37–44.

(23) Stearns, D. G. *J. Appl. Phys.* **1989**, *65*, 491–506.

(24) Holloway, K. L. Ph.D. Thesis, Stanford University, Palo Alto, CA, 1989.

**Table 2.** Summary of Samples Prepared<sup>a</sup>

sample no.	intended thickness (Å)		composn of Mo (%)
	Mo	Si	
A-1	5	32	19.1
A-2	5	32	20.1
A-3	5	23	22.71
A-4	5	17	23.68
A-5	5	24	24.01
A-6	5	17	24.64
A-7	5	22	25.89
A-8	5	23	27.65
A-9	3	10.5	29.69
A-10	3	9.75	30.73
A-11	3	9.5	30.45
A-12	5	17	31.28
A-13	3	10.0	31.81
A-14	3	9.25	35.05
A-15	3	9.5	35.23
A-16	3	10.5	35.87
A-17	5	10	39.44
A-18	5	9	46.63
A-19	5	8	51.71
B-1	5	9	55.41
B-2	7.5	8.0	60.18
B-3	8	6	62.3
B-4	7.5	6	63.12
C-1	5	4	65.79
C-2	10	5	70.29
C-3	10	6	73.14
C-4	10	5.6	73.74

<sup>a</sup> The layer thicknesses were measured using quartz crystal thickness monitors. The composition was measured using electron probe microanalysis. Compositions were within 5% of expected values.

from electron beam evaporation sources at a rate of 0.5 Å/s. Each source was independently monitored by quartz crystal thickness monitors. The thickness of each elemental layer was controlled to the nearest angstrom. The elemental composition of the samples were found to be repeatable to within about 5%. The films were simultaneously deposited on silicon and photoresist-coated silicon wafers. The silicon substrates were used for low-angle diffraction studies. The coated substrates were used to allow the sample to be removed from the substrate by soaking in acetone and collecting with Teflon filters.

Low-angle X-ray diffraction was used to characterize the multilayer periodicity and to study the interdiffusion of the elements. For samples with repeat spacings larger than 30 Å, diffraction maxima resulting from the elemental modulation was observed. High-angle X-ray diffraction was used to identify crystalline compounds. Copper K $\alpha$  radiation was used in the diffraction studies. The average composition of the multilayer films was determined by electron microprobe analysis using an energy-dispersive X-ray detector. Crystallinity of the samples was also examined using through foil TEM, where free-standing films were mounted on standard copper grids. The TEM used was a Phillips CM12 operated at an accelerating voltage of 100 keV.

Samples were annealed in a nitrogen atmosphere with less than 1 ppm oxygen. Substrate-free samples were annealed in a differential scanning calorimeter. Measured exotherms were correlated with X-ray and TEM results to identify and track the interdiffusion of the elements and the crystallization of any compounds.

## Results and Discussion

The samples prepared as part of this study are shown in Table 2. Large amounts of sample were required for the Kissinger analysis, resulting in the total thickness of the samples being on the order of 3000 Å. For many of the samples in Table 2, the sum of the intended layer thicknesses was below 20 Å and no low-angle diffraction maxima could be observed. This indicates that the films are rough, probably as a consequence of cumulative roughness building up during the deposition of 100–150 layers.<sup>31</sup> The roughness also prevents the observation

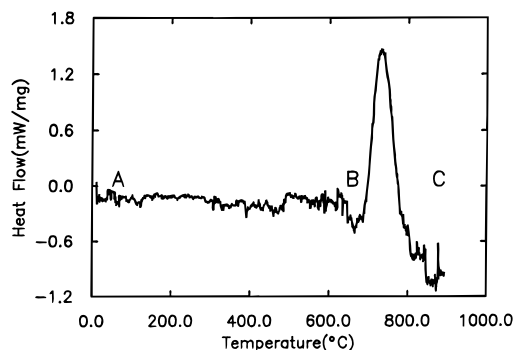


**Figure 1.** Differential scanning calorimetry data collected on a Mo:Si multilayer with composition near 3:1 Mo:Si. The temperature was scanned at 10 °C/min. The capital letters refer to annealing temperatures after which X-ray diffraction patterns were collected. These are shown in Figure 2.

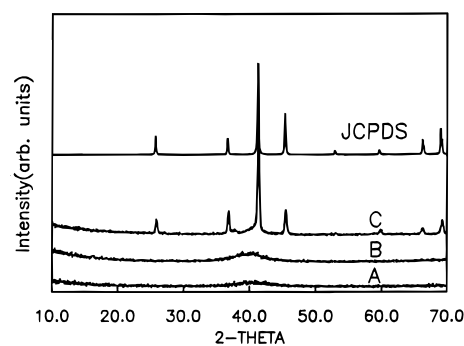
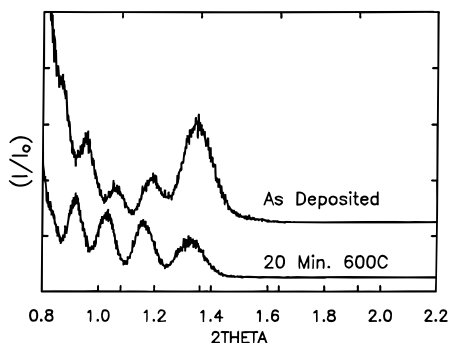


**Figure 2.** X-ray diffraction data collected as a function of annealing temperature on the Mo:Si multilayer with composition near 3:1 Mo:Si used in the DSC experiment shown in Figure 1. The scan labeled A was collected from an as-deposited sample, the scan labeled B was collected after annealing to 650 °C, and the scan labeled C was collected after annealing at 900 °C.

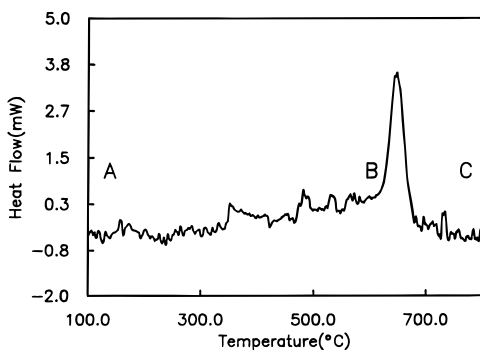
of the expected diffraction pattern resulting from the interference between the front and back of the deposited film. Films prepared with fewer layers or thicker repeat layer thicknesses contained the expected Bragg diffraction maxima as well as the expected high-frequency interference pattern from the front and back of the deposited films. To confirm that all of the prepared films contained molybdenum and silicon at the desired ratios, the composition was measured using electron microprobe analysis. The measured compositions of the samples are all within 5% of that expected from the ratio of the intended layer thicknesses. This rather large scatter results from shifts in the positions of the rate monitors during the time period in which the samples were prepared.

Figure 1 shows representative differential scanning calorimetry (DSC) data collected on a sample with composition near 3:1 Mo:Si. The heat flow as a function of temperature shows a sharp exothermic maxima near 720 °C. Diffraction data collected as a function of annealing temperature, shown in Figure 2, show that the diffraction pattern changes little during annealing below the exotherm temperature, containing only a broad diffraction maximum centered at approximately 40° 2 $\theta$ . On annealing the sample above 720 °C, the diffraction pattern is that expected from crystalline Mo<sub>3</sub>Si having the A-15 structure type. To determine what structural changes were occurring in the samples below the crystallization exotherm, low-angle diffraction data were collected as a function of annealing temperature for a sample with composition near 3:1 Mo:Si, as

(31) Fullerton, E. E.; Pearson, J.; Sowers, C. H.; Bader, S. D. *Phys. Rev. B* **1993**, *48*, 17432-17444.



**Figure 3.** Low-angle X-ray diffraction pattern collected on a Mo:Si multilayer with a repeat layer spacing of 75 Å and composition near 3:1 Mo:Si. The upper data were collected on the as-deposited sample, and the lower scan was collected after annealing the sample for 20 min at 600 °C.



**Figure 4.** Differential scanning calorimetry data collected on a Mo:Si multilayer with composition near 5:3 Mo:Si. The temperature was scanned at 10 °C/min. The capital letters refer to annealing temperatures after which X-ray diffraction patterns were collected. These are shown in Figure 5.

shown in Figure 3. These data clearly indicate that appreciable interdiffusion occurs at temperatures below the observed exotherm, confirming earlier observations. Surprisingly, there is little change in the high-order diffraction pattern indicative of crystal growth, while the elemental layers interdiffuse.

To further probe the evolution of the sample, transmission electron microscopy observations of representative samples were collected as a function of annealing. The through foil diffraction patterns obtained show that the films as deposited are amorphous, agreeing with earlier work by Sloof who investigated multilayers with repeat distances on the order of 10 Å or less.<sup>11</sup> Samples with total layer thicknesses less than 30 Å remained amorphous after extended annealing below the nucleation exotherm. Samples with total layer thicknesses greater than 30 Å but less than 100 Å show only the formation of small crystallites of Mo. No evidence for the formation of crystalline compounds, including Mo<sub>3</sub>Si, was found in the through foil TEM diffraction patterns of any of the samples. Annealing the samples above the exotherm temperature, however, clearly showed the formation of large grains of Mo<sub>3</sub>Si.

Similar experiments were performed on samples with compositions near that of the other stable molybdenum silicides present in the phase diagram. Thin multilayers prepared with compositions near 5:3 Mo:Si showed a sharp exotherm in the heat flow as a function of temperature near 650 °C, as shown in Figure 4. Diffraction data collected as a function of annealing, shown in Figure 5, and TEM data show that the samples are amorphous below the exotherm. Above the exotherm, the diffraction pattern is identical with that expected for Mo<sub>5</sub>Si<sub>3</sub>. Thin multilayers prepared with compositions near 1:2 Mo: Si

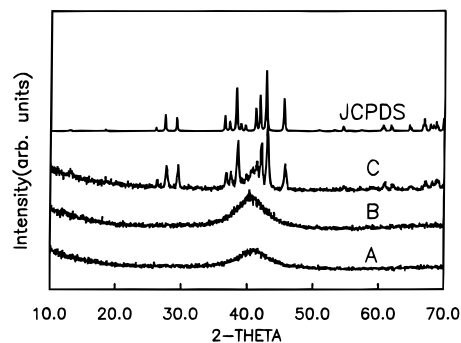


**Figure 5.** X-ray diffraction data collected as a function of annealing temperature on the Mo:Si multilayer with composition near 5:3 Mo:Si used in the DSC experiment shown in Figure 4. The scan labeled A was collected from an as deposited sample, the scan labeled B was collected after annealing to 600 °C, and the scan labeled C was collected after annealing at 750 °C.

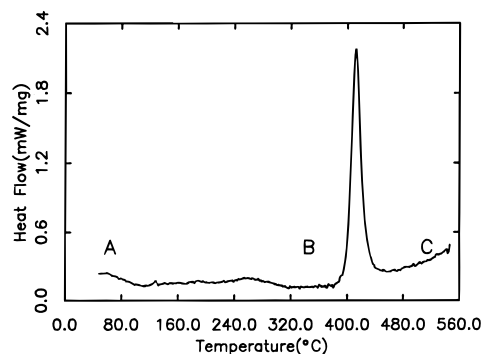


**Figure 6.** Differential scanning calorimetry data collected on a Mo:Si multilayer with composition near 1:2 Mo:Si. The temperature was scanned at 10 °C/min. The capital letters refer to annealing temperatures after which X-ray diffraction patterns were collected. These are shown in Figure 7.

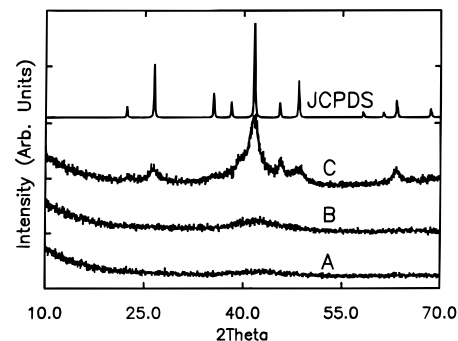


**Figure 7.** X-ray diffraction data collected as a function of annealing temperature on the Mo:Si multilayer with composition near 1:2 Mo:Si used in the DSC experiment shown in Figure 6. The scan labeled A was collected from an as deposited sample, the scan labeled B was collected after annealing to 350 °C, and the scan labeled C was collected after annealing at 550 °C.

showed a sharp exotherm in the heat flow as a function of temperature near 400 °C, as shown in Figure 6. Figure 7 contains diffraction data collected as a function of annealing for a representative sample. Below the exotherm temperature, the sample remains X-ray amorphous on annealing and through foil TEM studies confirm the samples are amorphous. Annealing above the exotherm temperature results in the formation of crystalline  $\beta$ -MoSi<sub>2</sub>.  $\beta$ -MoSi<sub>2</sub> is thermodynamically stable only above 1900 °C. The hexagonal  $\beta$ -MoSi<sub>2</sub> presumably forms because it is easier to nucleate than the low-temperature

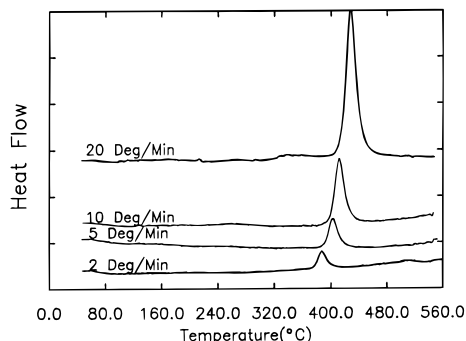


**Figure 8.** Differential scanning calorimetry data showing the shift in peak temperature for the exotherm as the heating rate is varied.

tetragonal form of  $\text{MoSi}_2$ . Heating to above  $700\text{ }^\circ\text{C}$  results in the conversion of the  $\beta$  phase to the thermodynamically stable  $\alpha$ - $\text{MoSi}_2$ .

The kinetic stability of the reaction intermediate present before the exotherm was studied by collecting differential scanning calorimetry data as a function of scan rate to estimate the activation energy of the nucleation and growth process. Such nonisothermal DSC data are typically analyzed using the method described by Kissinger<sup>32</sup> in which the activation energy can be obtained from the shift in peak temperature,  $T_p$ , as a function of scan rate,  $Q$ :

$$\frac{d \ln[Q/T_p^2]}{d[1/T_p]} = \frac{-E_{\text{crystallization}}}{R}$$

This equation is derived by assuming that the nucleation and growth can be described by the Johnson–Mehl–Avrami equation, that the initial and the final states have the same composition, and that the nucleation and growth rates are constant at constant temperature. A further approximation is made that both the nucleation rate and growth rates may be described by Arrhenius expressions over the range of temperature in which the peak temperature varies with the scan rate. Figure 8 shows the shift of the exotherm temperature as the scan rate was varied for a representative sample. Graphing  $\ln[Q/T_p^2]$  versus  $1/T_p$  gives a straight line with slope  $-E/R$ . Using this method of analysis gives an activation energy of 1.9 eV for a Mo:Si multilayer with composition near 1:2 Mo:Si. The diffraction data collected as a function of temperature suggest that this activation energy is associated with the nucleation and growth of  $\text{MoSi}_2$ . DSC data collected as a function of scan rate for a sample near 5:3 Mo:Si in composition was analyzed using Kissinger analysis, yielding an activation energy of 3.0 eV for the nucleation of  $\text{Mo}_5\text{Si}_3$ . An activation energy of 2.2 eV for the nucleation of  $\text{Mo}_3\text{Si}$  was determined for a sample with composition near 3:1 Mo:Si.

The results on the three samples discussed above are distinctly different from those previously reported in the literature for samples which contained thicker elemental layers. In these earlier studies, interfacial formation of binary compounds was observed and the identity of the interfacial compound formed was not a function of the overall composition. The data presented here suggest that these samples, consisting of much thinner elemental layers than studied previously, intermix without forming binary compounds at the reacting interfaces. If this hypothesis is correct, it implies that the exotherms result from the nucleation and growth of the observed compounds. To test this idea, we prepared a co-deposited sample with

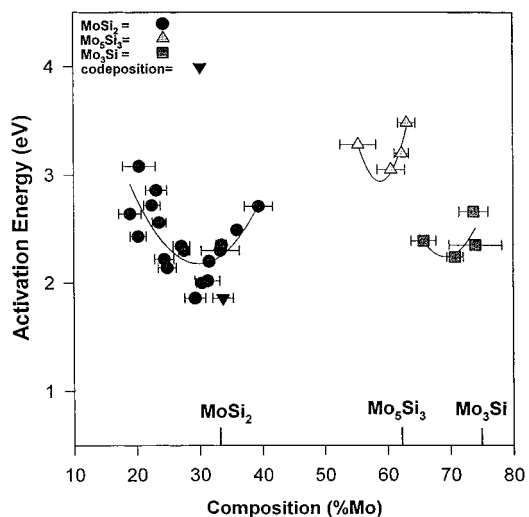


**Figure 9.** Activation energies, obtained using Kissinger analysis, plotted versus composition.

composition corresponding to the known binary compound  $\text{MoSi}_2$ . TEM of this sample indicated that it was amorphous as deposited. The co-deposited sample containing Mo and Si at a 1 to 2 ratio had an exotherm near  $400\text{ }^\circ\text{C}$ , very similar to the result obtained on the multilayered sample of the same composition. X-ray diffraction indicated that the sample was amorphous before the exotherm and had formed crystalline  $\beta$ - $\text{MoSi}_2$  afterward. The activation energy for the exotherm from this sample was 1.9 eV, within the experimental error of that determined from the multilayered samples of similar composition. This result supports the hypothesis that the samples interdiffuse before nucleating the compounds nearest in composition.

This result led us to measure the activation energy for nucleation and growth of each compound as a function of composition to probe the origin of the composition dependence of product formation. Figure 9 contains a graph of the measured nucleation energies as a function of composition. This figure clearly indicates that the origin of our ability to control product formation with composition is the composition dependence of the activation energy for nucleation. The variation of the nucleation energies with composition also supports the hypothesis that an amorphization reaction occurs leading to crystallization from a relatively homogeneous mixture of the respective elements.

Before discussing Figure 9 in more detail, it is useful to briefly review nucleation. The phenomena of nucleation arises from the interplay between energy terms dependent upon the surface and volume of an “embryo” of a thermodynamically more stable new phase forming from an existing phase. Since the new phase is more thermodynamically stable than the old phase, the energy per unit volume of the new phase is lower than that of the old. The energy decrease from the transformation is proportional to the volume of the new phase. There is also a surface energy term, however, describing the energy decrease due to increased stresses and decreased chemical bonding found at the interfaces. The relative magnitude of the surface energy and volume energy terms depend on the size of the particle, with the surface energy term dominating for small particles and the volume energy term dominating for large particles. There is a critical size above which the volume energy term dominates and the new phase

(32) Kissinger, H. E. *Anal. Chem.* **1957**, *29*, 1702–1706.

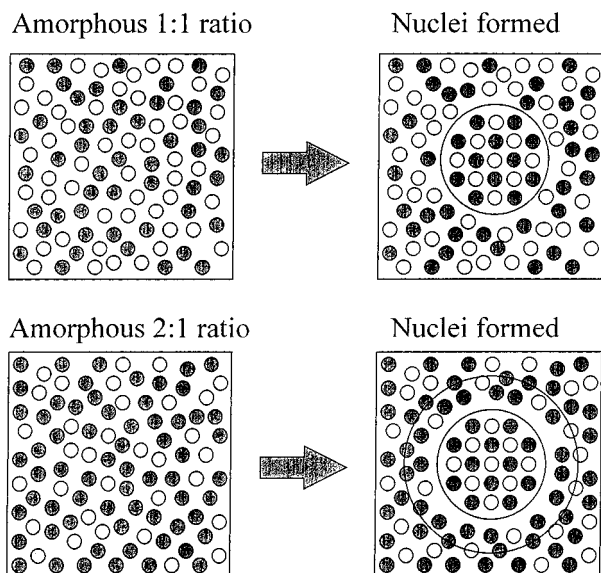


**Figure 10.** Schematic diagram of the structure of a nuclei showing the changes in volume and the disruption in bonding found at the surface of a critical nuclei. The upper figures show the change in structure around a critical nucleus formed from an amorphous intermediate of the same composition. The lower figure represents the case where the nuclei have a different composition from the amorphous intermediate. It is surrounded by a shell in which the composition is altered due to diffusion of the excess darkly shaded atoms out of the critical nuclei. spontaneously grows and a corresponding energy barrier associated with the formation of a particle of this critical size.<sup>33,34</sup>

The pronounced minima found in the composition dependence of the nucleation energy for the formation of all of the known binary compounds in Figure 9 result from the contribution of several factors which affect both the surface and volume energy terms. The volume energy term is a maximum at the stoichiometric compositions because off stoichiometry precursors must disproportionate to form a stoichiometric nuclei of the crystallizing compound. As a result, the free energy drop due to the formation of the stable phase is partially offset by the energy need to change the composition of the amorphous phase around the nucleus. In addition, the surface energy term also depends on the composition of the amorphous phase relative to that of the phase being crystallized. The surface energy term has a "mechanical" energy component which depends on the change in volume of the nuclei relative to the amorphous precursor. In addition, the surface energy term has a component resulting from discontinuities in bonding between the nuclei and the amorphous matrix. In the case where the amorphous precursor has a different composition from that of the crystallizing phase, the surface energy term is likely to be larger as a result of disproportionation. The atoms diffusing out of the nucleus will affect the volume and bonding in a shell shaped region of space around the nuclei. The shell shaped region will be enriched in the diffusing species, affecting the bonding within the shell, between the shell and the nuclei, and between the shell and the surrounding amorphous background. As shown schematically in Figure 10, the total surface area of the region perturbed by the forming nuclei is much larger than that found in the stoichiometric case.

While we believe that this and a previous study of the formation of InSe<sup>29</sup> are the first measurements of the composi-

(33) Strey, R.; Wagner, P. E.; Viisanen, Y. *J. Phys. Chem.* **1994**, *98*, 7748–7758.

(34) Brophy, J. H.; Rose, R. M.; Wulff, J. *The Structure and Properties of Materials*; John Wiley & Sons, Inc.: New York 1964; Vol. 2, pp 98–108.

tion dependence of the nucleation energy, it has long been recognized that the kinetic stability of amorphous glasses is strongly dependent on composition. The kinetic stability of glasses is greatest when their composition is furthest from the stoichiometries of known compounds.<sup>35</sup> In agreement with this general observation, there were no exotherms observed for samples greater than 40% Mo and less than 50% Mo. These samples were still amorphous with respect to X-ray diffraction after annealing at 600 °C. TEM data confirmed that they were still amorphous after annealing at 600 °C. After annealing at 800 °C, TEM studies show that the samples consist of a mixture of crystalline MoSi<sub>2</sub> and Mo rather than a mixture of MoSi<sub>2</sub> and Mo<sub>5</sub>Si<sub>3</sub> as expected from the phase diagram. This supports the assertion that nucleation of the crystalline compounds is the rate-limiting step in product formation. The phases which crystallize are the easiest phases to nucleate, not necessarily those which are thermodynamically most stable.

For all three compounds the minimum activation energies are shifted to the more silicon rich side of the stoichiometric composition. We speculate that this shift is a result of higher average interdiffusion rates for silicon rich compositions. The amorphous intermediates are kinetically stable because they are diffusionally constrained. Higher interdiffusion rates allow the system to sample different configurations at a higher rate, thus increasing nucleation rates.

The widths of the minima in Figure 9 vary depending on the compound crystallized. Although there is considerable scatter in the data, the width of the minimum for the composition dependence of nucleation of Mo<sub>5</sub>Si<sub>3</sub> is narrower than that of Mo<sub>3</sub>Si which is similar in width to that observed for MoSi<sub>2</sub>. The width of the minima should depend on the size of the critical nucleus which might be expected to scale with the complexity of the crystal structure. Simple structures which are very close in bonding and atomic distribution to the amorphous surroundings can be easily obtained by minimal rearrangement of the amorphous intermediate. More complex structures, however, will need to undergo fluctuations in local energies and densities which are further removed from that of the surrounding amorphous material. This is consistent with our observations in that the widths of the minima scale with the number of atoms in the unit cell of the crystallizing compound. The high-temperature form of MoSi<sub>2</sub> which nucleated directly from the amorphous intermediate has a hexagonal structure ( $a = 4.64$  Å,  $c = 6.53$  Å) with nine atoms in the unit cell and Mo<sub>3</sub>Si has the cubic A-15 structure ( $a = 4.897$  Å) with eight atoms in the unit cell. Mo<sub>5</sub>Si<sub>3</sub> has a much more complicated tetragonal structure ( $a = 9.643$  Å,  $c = 4.910$  Å) with thirty-two atoms in the unit cell. The magnitude of the activation energy also scales with the number of atoms in the unit cell with MoSi<sub>2</sub> and Mo<sub>3</sub>Si having nucleation energies considerably less than Mo<sub>5</sub>Si<sub>3</sub>. This increase in activation energy is consistent with an increase in the size of the critical nucleus with increasing complexity of the crystal structure. A larger critical nucleus requires a larger composition fluctuation which is energetically more difficult.

## Conclusions

Elementally modulated reactants form amorphous intermediates if the repeat layer thickness is below some critical value. In the molybdenum–silicon system investigated in this article, amorphous intermediates were formed when the sum of the molybdenum and silicon layer thicknesses in the repeating

(35) Beck, H.; Güntherodt, H.-J. In *Glassy Metals I: Ionic Structure, Electronic Transport, and Crystallization*; Beck, H., and Güntherodt, H.-J., Eds.; Springer-Verlag: New York, 1981; Vol. 46; pp 1–17.

bilayer were less than 20 Å for metal rich samples and less than 40 Å for silicon rich samples. The composition of the amorphous intermediate was shown to control nucleation of the binary molybdenum silicides. The variety of compounds observed to be the first compound formed at a reacting molybdenum–silicon interface in the literature may be a result of composition variations in the amorphous interlayer region between the Mo and Si before crystalline products form.

The data presented in this paper show why composition can be used to control nucleation from amorphous reaction intermediates. The nucleation energy as a function of composition contains minima for each compound in the phase diagram. This provides a rational understanding for the formation of the thermodynamically unstable compounds using this synthetic approach.<sup>36</sup> To prepare a thermodynamically unstable compound, one “just” needs to make its nucleation energy smaller than that of other possible compounds in the phase diagram under investigation. Composition is one parameter which can be used to control relative nucleation energies.

The results presented in this manuscript have important implications for the synthesis of new compounds in ternary and

higher order systems. These results suggest that one can avoid forming binary compounds and nucleate ternaries directly by taking advantage of the composition of an amorphous intermediate. This ability to avoid thermodynamically more stable compounds through control of reaction intermediates becomes significantly more important in ternary and higher order systems. If one can avoid the formation of thermodynamically stable binary compounds as reaction intermediates, the number of new compounds which can be prepared dramatically increase.<sup>37</sup> The results presented here suggest that in systems in which an amorphous intermediate can be obtained, the concentration of the ternary atom in the amorphous intermediate can increase in the nucleation energy of binary compounds, making the activation energy of possible ternary compounds lower relative to the competing binaries.

**Acknowledgment.** The support of the National Science Foundation (Grant DMR-9510562) is gratefully acknowledged.

JA9802302

---

(36) Hornbostel, M. D.; Hyer, E. J.; Thiel, J.; Johnson, D. C. *J. Am. Chem. Soc.* **1997**, *119*, 2665–2668.

---

(37) Brewer, L. *J. Chem. Educ.* **1958**, *35*, 153.

(38) Chi, E.; Shim, J.; Kwak, J.; Baik, H. *J. Mater. Sci.* **1996**, *31*, 3567–3572.